Design and Experimentation of Additively Manufactured Hierarchical Architected Lattices for Energy Absorption

Presented in Partial Fulfillment of the Requirements for Graduation with Honors Research Distinction in the Department of Mechanical and Aerospace Engineering at The Ohio State University

By

Mohamad Al Nashar

The Ohio State University

Honors Undergraduate Program in Mechanical Engineering

April 2020

Thesis Committee:

Professor Alok Sutradhar, Advisor

Dr. Sandra Metzler

ABSTRACT

Energy absorption structures are critical components in many engineering applications, such as sport equipment and transportation crashworthiness. Conventional energy absorption structures such as foams and lattices have demonstrated their effectiveness and strengths, however, they lack the significant design degrees of freedom that 3D hierarchical architected lattices possess. This research aims at expanding the design domain of energy absorption lattices, and aids future work in design optimization of energy absorption lattices.

This research investigates the energy absorption capabilities of 3D hierarchical architected lattices. Hierarchical lattices are structures composed of self-similar or different architected metamaterials across multiple length-scales. Hierarchical architected lattices have superior properties when compared to conventional homogeneous materials; and opens the door for a wide range of material property manipulation and optimization.

The effect of introducing a hierarchy to a lattice on the energy absorption performance is demonstrated. In addition, the effect of relative density on the energy-absorption was isolated by creating a comparison between a 1st order Octet lattice that has the same relative density as a 2nd order Octet lattice. The effect of changing the 2nd order unit cell geometry from an Octet, Dodecahedron, to Truncated Octahedron is studied. The results will establish a series of trends related to energy-absorption capacity, volumetric energy-absorption efficiency, load, and strain applied. The effect of changing the cross-sectional geometry of the trusses with respect to energy-absorption performance is investigated. Changing the orientation of the 2nd order cells has a considerable effect on the force displacement-curve, and the energy-absorption performance of the lattice. An analytical solution for the 1st order and the 2nd order Octet lattices is discussed to the validate the force-displacement results obtained from the finite element analysis. In addition, in order to compare the force-displacement

behavior of the 1st and the 2nd order Octet lattices, an experimental compression test mimicking the finite element analysis boundary conditions was conducted. The findings and the provided comprehension of this research will aid the future work in optimization of energy-absorption architected lattices.

ACKNOWLEDGEMENTS

First, and most of all, I would like to thank Professor Sutradhar for the opportunity to work on this extraordinary project, his guidance, and assistance throughout the project and the process of writing this thesis. I would like to express my appreciation to my other committee member Dr. Metzler for her valuable feedback, support, and encouragement.

I'm extremely grateful for my lab partners Tareq Zobaer, Sourav Das, and Teck Koh for their constant support and help throughout this journey, in the early mornings, and late nights.

Last, but not least, I would like to thank my parents for their continuous support, and unbounded love throughout my college career. Without their support, my work wouldn't be possible.

TABLE OF CONTENTS

ABSTRACT 3
ACKNOWLEDGEMENTS 5
LIST OF FIGURES 7
LIST OF TABLES 8
LIST OF ABBREVIATIONS 9
CHAPTER I: INTRODCUTION 10
1.1 Background and Literature 10
1.2 Objective and Significance 15
1.3 Thesis Overview 16
CHAPTER II: METHODOLOGY 17
2.1 Hierarchical Structure Generation 17
2.2 FEA Setup 20
2.3 Fabrication Procedure 23
2.4 Experimental Testing Setup 24
CHAPTER III: FEA RESULTS AND DISCUSSION 25
3.1 Effect of Hierarchical Order on Energy Absorption 25
3.2 Effect of H2 Unit Cell Geometry on Energy Absorption 27
3.3 Effect of H2 Unit Cell Orientation on Energy Absorption 32
3.4 Effect of H2 Cross-Sectional Geometry of Trusses 33
3.5 Analytical Solution 35
3.6 Experimental Testing 36
CHAPTER IV: CONCLUSION AND FUTURE WORK 39
BIBLIOGRAPHY 41
APPENDIX 43
A. FEA Stress Contour Plots 43
B. Geometric Parameters of Truss Cross-Sections 45

LIST OF FIGURES

Figure 1: Classification of cellular materials 10
Figure 2: Basic unit cell classification 11
Figure 3: Relationship between relative density and energy absorption 12
Figure 4: Classification of Hierarchical order of an Octet lattice 15
Figure 5: Methodology flowchart 17
Figure 6: 1st order Octet unit cell 17
Figure 7: Design of 2nd order unit cell 18
Figure 8: Orientation of 2nd order unit cells with respect to XY plane 18
Figure 9: Unit cells used in the 2nd hierarchy 19
Figure 10: 2nd order lattices 19
Figure 11: Geometric description of a 2nd order lattice 20
Figure 12: Stress-strain curve of TPU material 22
Figure 13: FEA material model comparison of linear elastic versus calibrated model using stress-strain data 23
Figure 14: SLA 3D printing 24
Figure 15: Compression testing using an Instron machine 24
Figure 16: Effect of hierarchical order on energy absorption 25
Figure 17: Effect of 2nd order unit cell geometry on Energy absorption 27
Figure 18: Maximum von mises stress in three H2 lattices 29
Figure 19: FEA Von mises stress contours, (a) H2 Trunc.Octa, (b) H2 Octet , (c) H1 Octet , (d) H2 Dodecahedron 30
Figure 20: Effect of 2nd order cell orientation on energy absorption 32
Figure 21: Effect of truss cross-sectional geometry on energy absorption 33
Figure 22: Ratio of stiffness between H1 and H2 Octet (Analytical and FEA) 36
Figure 23: Experimental force-displacement curve of H1 Octet 37
Figure 24: Experimental and simulation (linear) plots of H2 Octet 38

LIST OF TABLES

Table 1: ABAQUS FEA Setup 21
Table 2: Effect of hierarchy on energy absorption 26
Table 3: Energy absorption and volumetric efficiency of hierarchical lattices @ 15 N 28
Table 4: Volumetric efficiency factors at 50% strain of hierarchical lattices 29
Table 5: Summary of stiffness, magnitude of the dip ΔF, and Volumetric energy absorption efficiency η for various truss cross sectional geometries on a H2 Octet lattice 34
Table 6: Parameters of analytical solution 35

LIST OF ABBREVIATIONS

B31	2-node linear beam element in space
B32	3-node quadratic beam element in space
BCC	Body-centered cubic
B-rep	Boundary representation
F	Compressive or transmitted Force
FCC	Face-centered cubic
FEA	Finite element analysis
H1	First order lattice
H2	Second order lattice
H2 45d	Second order lattice with 45-degree orientation
SC	Simple cubic
SLA	Stereolithography
S,mises	Von mises stress
TPU	Thermoplastic polyurethane
Trunc.Octa	Truncated Octahedron
W	Work or Energy

CHAPTER I: INTRODCUTION

1.1 Background and Literature

During impact scenarios, we often seek to protect a piece of machinery, a structure, or ourselves; from the destructive effect of the transmitted force that can have a negative impact on the body that is being hit. Scientist and engineers have always been looking for ways to absorb impact energies efficiently, and over a wide range of impact intensities [1]. Energy absorption is an important field that affects many industries and has critical applications. In the transportation industry, important applications are crashworthiness of vehicles [4], and crashworthiness of airplane fuselage [5]. Important applications in the sports industry are the midsole and insole in running shoes for comfort [2], and extreme-sports helmet cushioning for safety [3]. These needs have been mostly addressed by using cellular materials or composite materials when designing protective structures.

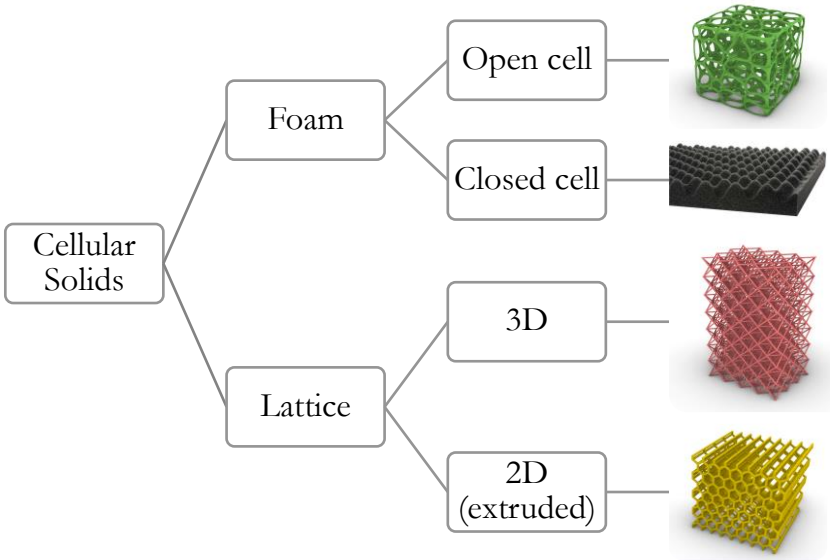

Figure 1: Classification of cellular materials [6]

In general, cellular materials can be classified into two main categories as seen in Figure 1. *Foams and lattices* [6]. **Foams** have shown to achieve good energy absorption performance. Foams are composed of internal cellular structures that can collapse and dissipate energy. In general, foams can be categorized as either open cell foams or closed cells foams [6]. Closed cell foams can absorb energy through the crumbling action of internal cells and the compression of internal air trapped inside the cells. Open cells can dissipate energy through cell collapsation and the action of air displacement [6]. Various parameters that can affect the energy absorption capabilities of foams have been investigated [7][8]. One of the most important features that can be controlled in foams is the gradient density across the foam, by changing the density gradient function across the foam, one can alter the optimized range of energy absorption, the logarithmic density gradient stands as the best density gradient for impact energy absorption when compared to linear, cubic and square root density gradient functions [7]. Having a density gradient allows the foam to efficiently absorb the impact energy over a wider range of loads [7]. Another important factor is the density of the foam. Lower density foams tend to have lower plateau stress, and as a result, the flat plateau region occurs at an earlier stage. Whereas a higher density foam tends to have a higher plateau stress, and consequently, the flat plateau region occurs at a later stage [8].

Lattice structures stand as another option for energy-absorption applications. Truss-based structures or lattices can take many forms. The most known cell configurations for lattices are simple cube, body center cubic (BCC), and face centered cubic (FCC) shown in Figure 2 [Source: Wikipedia, Cubic Crystal System].

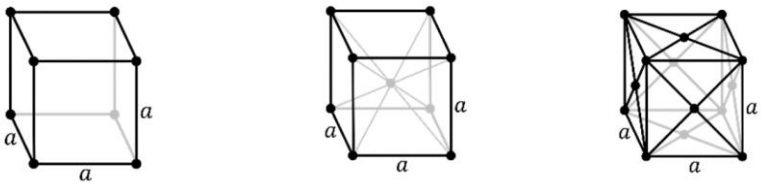

Simple cube (SC) Body-centered cubic (BCC) Face-centered cubic (FCC)

Figure 2: Basic unit cell classification [Source: Wikipedia, Cubic Crystal System]

A lot of studies have been done on the topic of energy absorption capabilities of lattices [19][20][21][22]. The lattice unit cells are typically designed to harness instabilities and maximize buckling, thus, maximizing energy absorption [9],[16]. Similar to foams, the density affects the energy absorption capacity of the lattice [10]. On the other hand, lattices offer more design degrees of freedom when compared to foams; which allows the designer to tailor their design to a specific impact scenario [3]. Whereas foams are characterized by a chaotic structure (stochastic), therefore their behavior is harder to predict.

For both lattices and foams, the energy absorption capacity is calculated as the area under the curve of a stress-strain curve or a force-displacement curve.

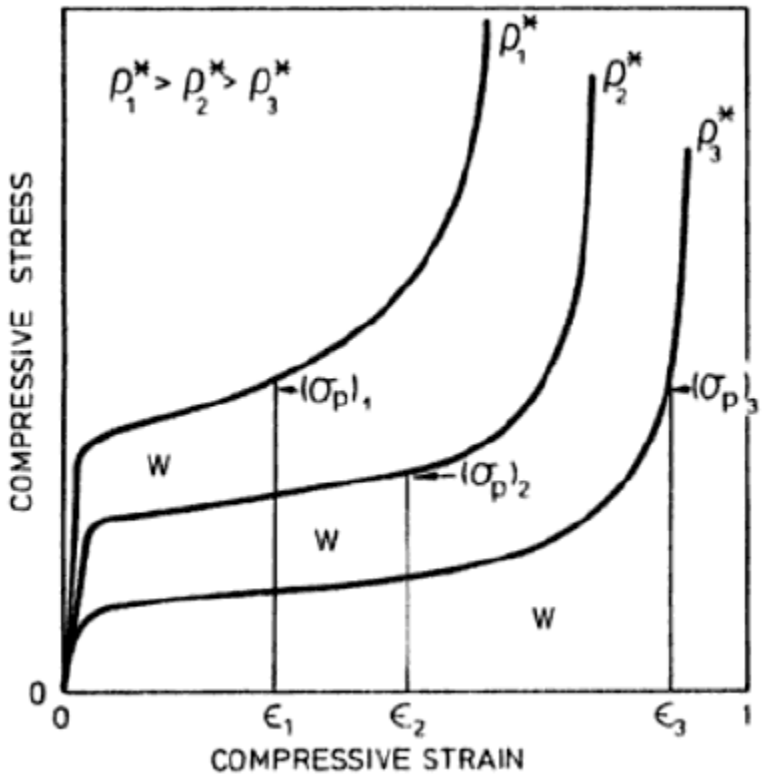

Figure 3: Relationship between relative density and energy absorption of cellular solids [6]

Typical trend between the relative density of the structure and its energy absorption capacity under compression for cellular materials has been explored previously [8], and can be seen in Figure 3 above. The relative density of cellular materials is defined as $\frac{\rho}{\rho_s}$, where ρ_s is the density of the solid material, and ρ is the density of the structure of interest.

The initial slope (stiffness) of the stress-strain curve or the force-displacement curve depends mostly on the material properties. However, the length of the plateau flat region and when it occurs depends on the relative density, geometry of the structure, and the strain rate [6]. In addition to the area under the curve calculations, a volumetric energy-absorption efficiency factor was introduced in the literature. The volumetric efficiency factor is defined as the ratio of the area under the force-displacement curve (energy absorbed) divided by the maximum transmitted force [3]. The efficiency factor is introduced in order to normalize the energy absorption quantity, and compare the energy absorption performance of different lattices.

In dynamic impact scenarios, inertia and time depended material behavior are prominent effects; thus, it's important to distinguish between low, intermediate, and high strain rates. Low strain rates have impact velocities below 10 m/s, intermediate strain rates have impact velocities between 10 m/s to 50 m/s, while high strain rates have impact velocities higher than 50 m/s [15]. Moreover, during an impact, the resultant acceleration and its duration are important parameters. These parameters have big implications in the head protection industry as many head injury criteria rely on acceleration durations as indicators of the likelihood for a person suffering significant head trauma [7][23][24].

In an effort to expand on lattices and provide a wider selection for the designer to obtain optimized designs, this research will introduce the concept of hierarchical structures in lattices, and investigate their energy absorption performance. Hierarchical structures are a bio-inspired design that can be incorporated in foams or lattices in order to enhance the energy absorption capability [11][17].

Hierarchical structures are first observed in nature, both in macro and micro scales. Among the foremost representative examples of fruits in nature is the pomelo fruit. The citrus fruit is a native of South America and can withstand falls of up to 10 meters high and to preserve its integrity [12]. On the other hand, man-made hierarchical structures such as the well-known Eiffel tower, incorporates a hierarchy to reduce its weight and optimize its structural integrity. Cables used in suspension bridges are composed of different wire diameters, strands, twist angles at different lengths scales to optimize its strength or fatigue durability. The design optimization of the cable depends on the placement of the cable in the bridge, and the cable's function.

Recent literature has discussed the potential capabilities of hierarchical structures [11][13][18]. A 2D hierarchical tubular structure inspired by tendon was investigated in terms of energy absorption capabilities and showed a 73% improvement in energy-absorption performance when a hierarchy is introduced [11]. The performance of the hierarchical structure has shown to be sensitive to key design parameters such as velocity of impact, mass of impactor and wall thicknesses of tubes [11]. Further analyses showed that there is a greater reduction in maximum von mises stresses with lower relative density [11]. The effect of introducing a hierarchy on mechanical properties such as stiffness has also been investigated by recent studies. For example, the specific stiffness and strength values of hierarchical lattices decrease exponentially with the increase in hierarchical order [13],[18]. Moreover, among the Octet, Tetrakaidekahedron, and Cuboctahedron unit cells; a hierarchical lattice with a combination of a first order Octet and a second order Octet has yielded the highest stiffness [18]. Figure 4 is a classification of an Octet hierarchical unit cell [18].

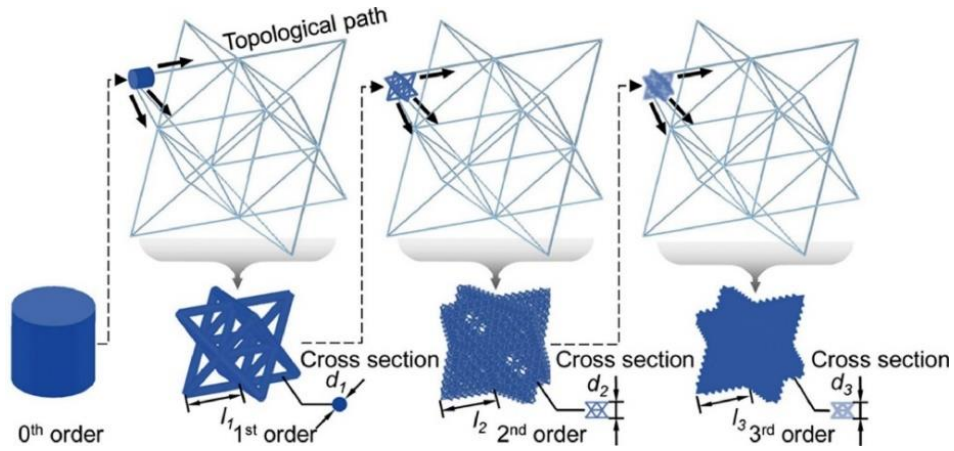

Figure 4: Classification of Hierarchical order of an Octet lattice [18]

1.2 Objective and Significance

While previous studies in lattices and foams for energy absorption have demonstrated their effectiveness and strengths, the subject of energy absorption capabilities of 3D hierarchical lattices remains to be fully understood. This research will implement the concept of hierarchical structures and study the energy absorption capabilities of 3D hierarchical lattices. Such engineered structures have complex geometric topologies, and because of the advancements in the additive manufacturing field, such designs are now attainable.

We choose lattices over foams as our host for hierarchical structures, due to the fact that lattices offer more design degrees of freedom when compared to foams; which allows us to tailor our design to specific impact scenarios [3]

In this project, the base 1st order structure is an Octet unit cell, while we vary the geometry of the 2nd order unit cells. Parameters such as the unit cell geometry of the 2nd order, the cross-sectional geometry of the trusses, and the orientation of the 2nd order unit cells will be explored.

1.3 Thesis Overview

This thesis holds four chapters. The first chapter embraces the background, literature, objective and the significance of this research. Chapter II covers the methodology of this research that includes the design procedure, the FEA setup, the material characterization discussion, the fabrication method, and the experimental testing setup. Chapter III contains the FEA results and discussions, followed by an analytical solution for verification, and at the end, the experimental test data will be analyzed. Chapter IV concludes with all the findings and the results on the energy absorption capabilities of 3D hierarchical lattices, and discusses the trends observed with respect to the studied parameters.

CHAPTER II: METHODOLOGY

The methodology of this project encompasses four main pillars (section 2.1-2.4), demonstrated in Figure 5. Section 2.1 will discuss the design procedure. Section 2.2 will explain the FEA setup and discuss the material model used in the simulations. Section 2.3 will go over the fabrication method. Section 2.4 will discuss the experimental setup for the compression test.

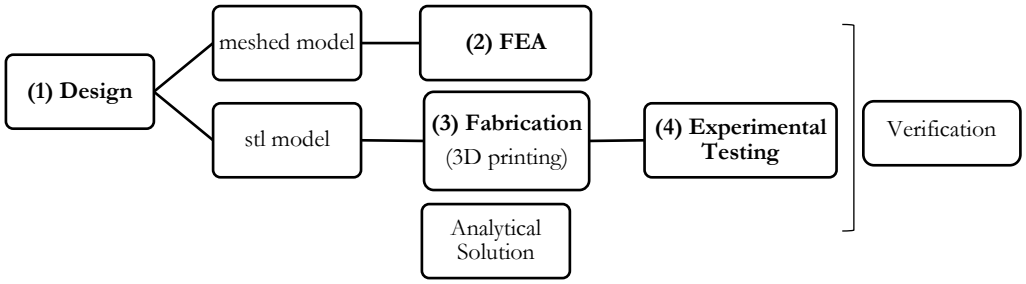

Figure 5: Methodology flowchart

2.1 Hierarchical Structure Generation

Hierarchical lattices are structures composed of self-similar or different architected unit cells across multiple length-scales. In order to construct such structures, a parametric modeling design tool (Rhinoceros 3D) is used to generate the models. The design process starts with the design of the 1st order unit cell as a wireframe connecting the nodes of the unit cell as seen Figure 6.

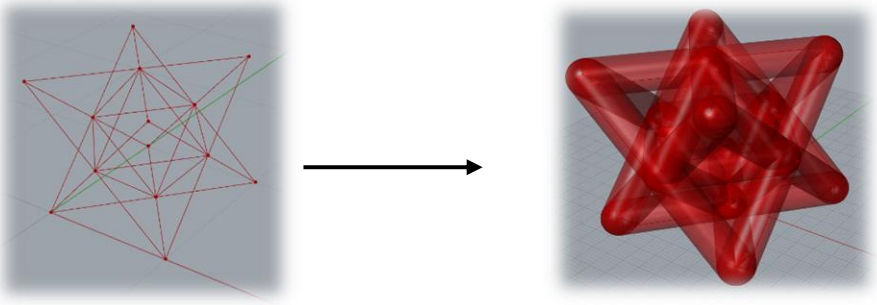

Figure 6: 1st order Octet unit cell

The wireframe of the 1st order is then given a thickness in the form of a pipe of an adequate diameter to generate a B-rep model. The diameter of the 1st order lattice dictates how big the design space is for the 2nd order cells. The resultant 1st order unit cell B-rep is utilized as the design space for the 2nd order cells. The output of the generation process is a 2nd order wireframe lattice. The wireframe can be converted again to a B-rep by generating a thickness in the form of a solid pipes (figure 7b,7c).

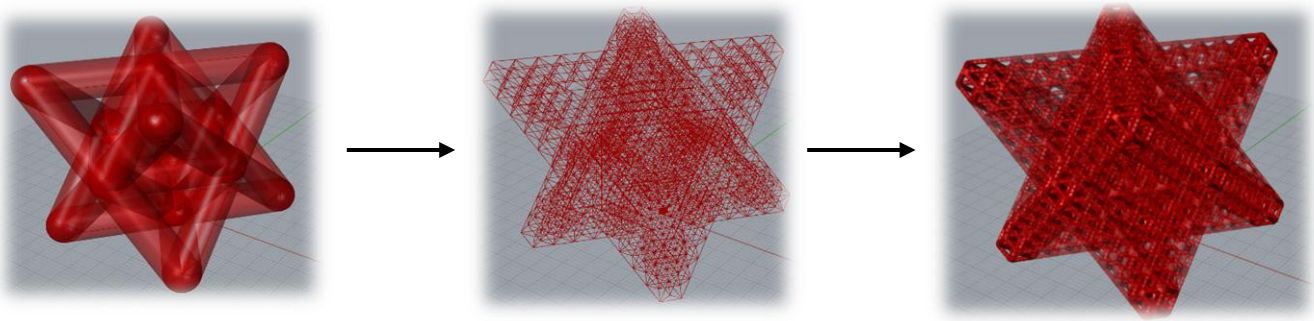

(a) (b) (c)

Figure 7: 2nd order Octet unit cell, (a) 1st order Octet [B-rep], (b) 2nd order wireframe, (c) 2nd order Octet [B-rep]

The parametric design tool allows the user to change the orientation of the 2nd order cells relative to the XY plane. For example, changing the orientation of the second order Octet cells 45 degrees will result in a different structure shown below in Figure 8.

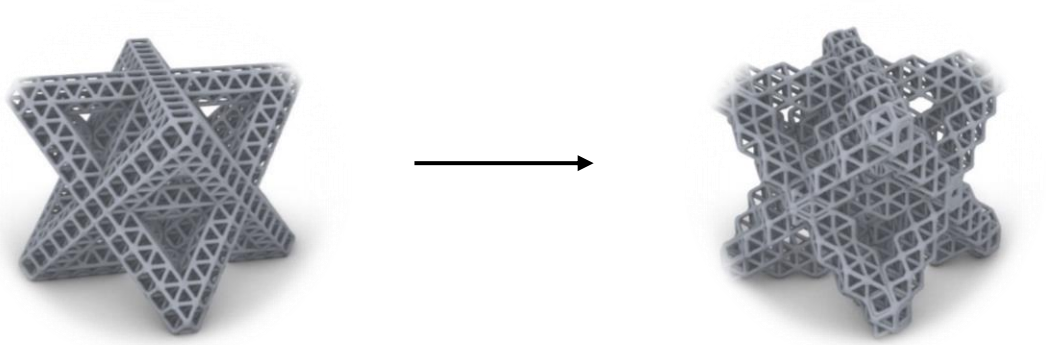

(a) (b)

Figure 8: Orientation of 2nd order unit cells with respect to XY plane, (a) 2nd order Octet, (b) 2nd order Octet 45d

The same approach can be followed for different second order unit cells. For this study, the base 1st order lattice will be an Octet. The 2nd order cells that will be investigated vary from an Octet, Dodecahedron, to Truncated Octahedron unit cells. The unit cell geometries are shown in Figure 9 below. In addition, the corresponding 2nd order lattices are shown below in Figure 10.

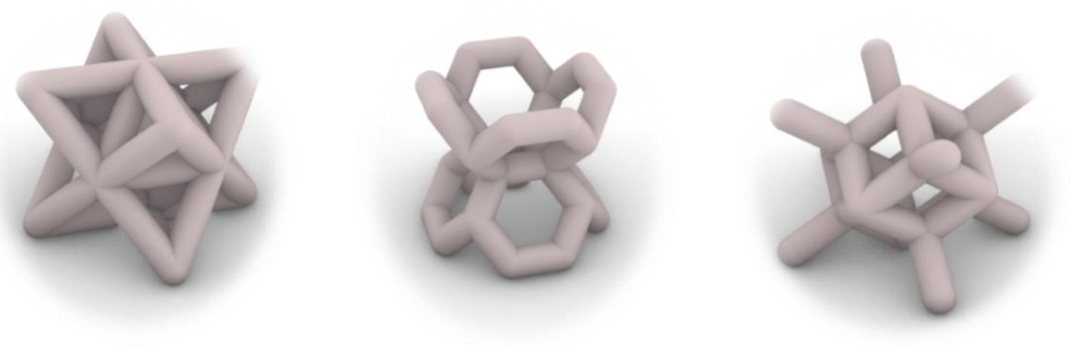

(a) **(b)** **(c)**

Figure 9: Unit cells used in the 2nd hierarchy, (a) Octet, (b) Truncated Octahedron, (c) Dodecahedron

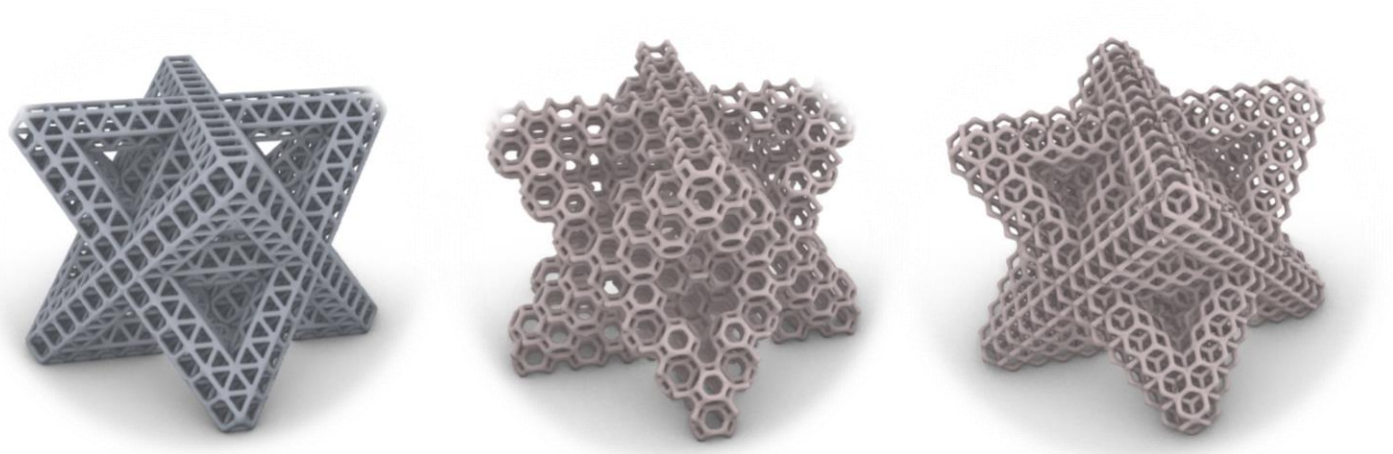

(a) **(b)** **(c)**

Figure 10: 2nd order lattices, (a) H2 Octet, (b) H2 Trunc.Octa, (c) H2 Dodecahedron

The geometric description for this study is kept constant throughout the various designs, and the geometric parameters of the 2nd order unit cells (truss diameter, number of elements across L, volume of design space) were maintained the same across all designs. This is summarized in Figure 11 below.

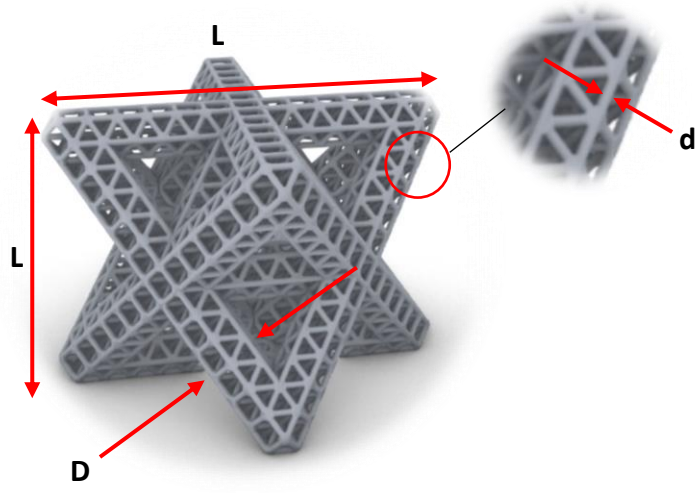

Geometric Description	
D	6.25 mm
d	1 mm
L	40 mm

Figure 11: Geometric description of a 2nd order lattice

2.2 FEA Setup

To observe the effect of the structure's hierarchical order on the energy-absorption performance, lattice models were imported to simulate a compression scenario of a rigid plate pressing against the lattices using ABAQUS. Dynamic explicit analysis was used for the 2nd order lattice to incorporate geometric nonlinearity that could result from a buckling scenario; whereas implicit analysis was sufficient to simulate the 1st order lattice. Instead of using solid continuum elements, beam elements were used in this project due to their computational efficiency. On the other hand, when compared to other simplified elements such as truss elements, beam elements can account for bending moments in addition to axial loadings. Table 1 below summarizes the parameters used for each simulation. For all simulations, it was sufficient to apply a hard contact condition with a 0.3 friction penalty between the two rigid plates and the deformable lattice for the simulations to converge. The boundary conditions were applied at two reference points, each point constrained to each of the rigid plates. The bottom plate is assigned a fixed boundary condition, while the top plate is displaced 20 mm in the vertical direction in order to cause a 50% overall lattice strain. For the purpose of obtaining

consistent and comparable results, the same approach and boundary conditions were applied to the rest of second order lattices of interest.

Table 1: ABAQUS FEA Setup

Parameter	**1st Order**	**2nd Order**
Material properties	TPU, E=12 MPa, density 1.12 g/cc	
Pipe diameter	6.25 mm	1 mm
Impact velocity	20 mm/s	
Mesh element type	B31 (2-node linear beam element)	B32 (3-node quadratic beam element)
Number of elements	396	28752
Analysis type	Implicit	Explicit
Loading condition	50% strain	

In order to decide what material model to use in the finite element analysis, a material characterization study was done on the polyurethane (TPU) material by conducting a tensile test of a dog bone specimen. The specimen is loaded in tension until failure (ultimate strength). Figure 12 below demonstrates the polyurethane (TPU) stress-strain curve and its important regions.

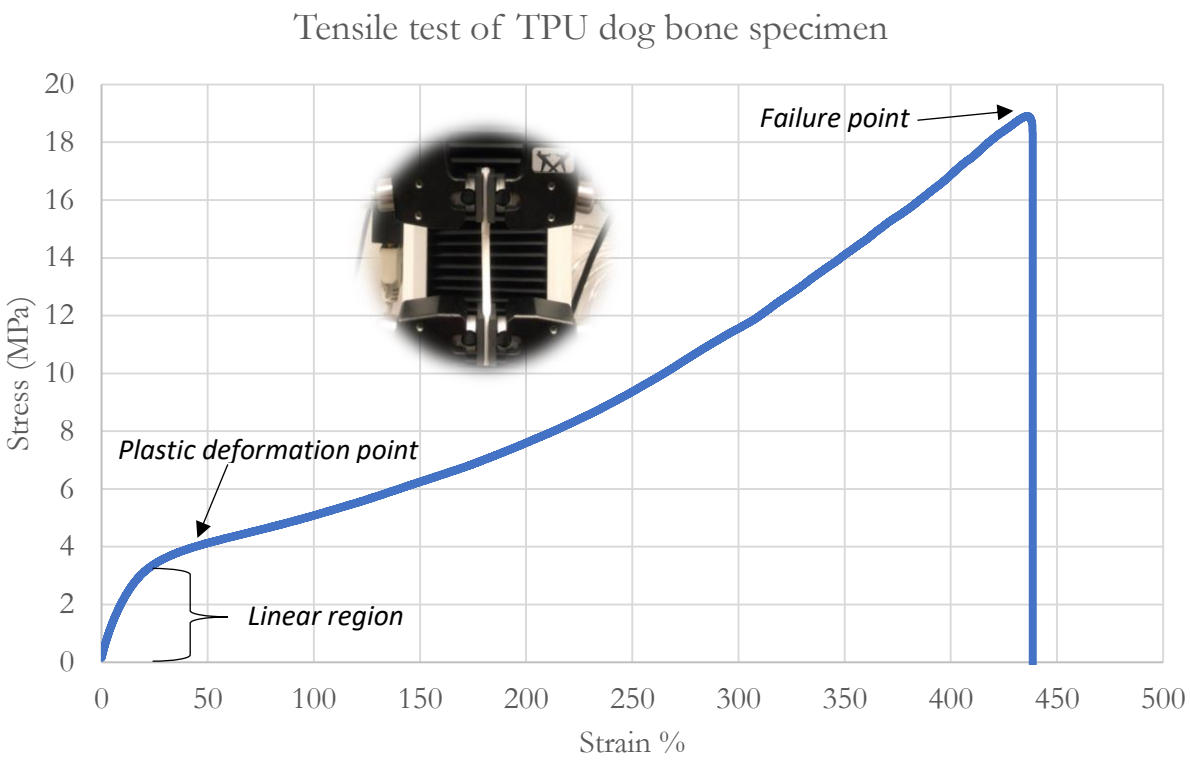

Figure 12: Stress-strain curve of TPU material

It was observed that for the low stress region, the behavior can be approximated as linear elastic. In the case of the investigated lattices, the von mises stresses observed in the FEA simulation (Appendix A1-A5) correspond to the low stress region (0 MPa - 4 MPa) in the material model curve, thus, one can deduce that if nonlinearity exists, its due to the boundary conditions (CONTACT) and the geometry (buckling). Figure 13 demonstrates the difference between the linear model and a calibrated model using experimental stress-strain data in ABAQUS. A small difference between the two models starts to appear over large displacements, this is where the stresses in the model get close to the plastic yielding point shown in Figure 12, where it starts to behave in a nonlinear fashion.

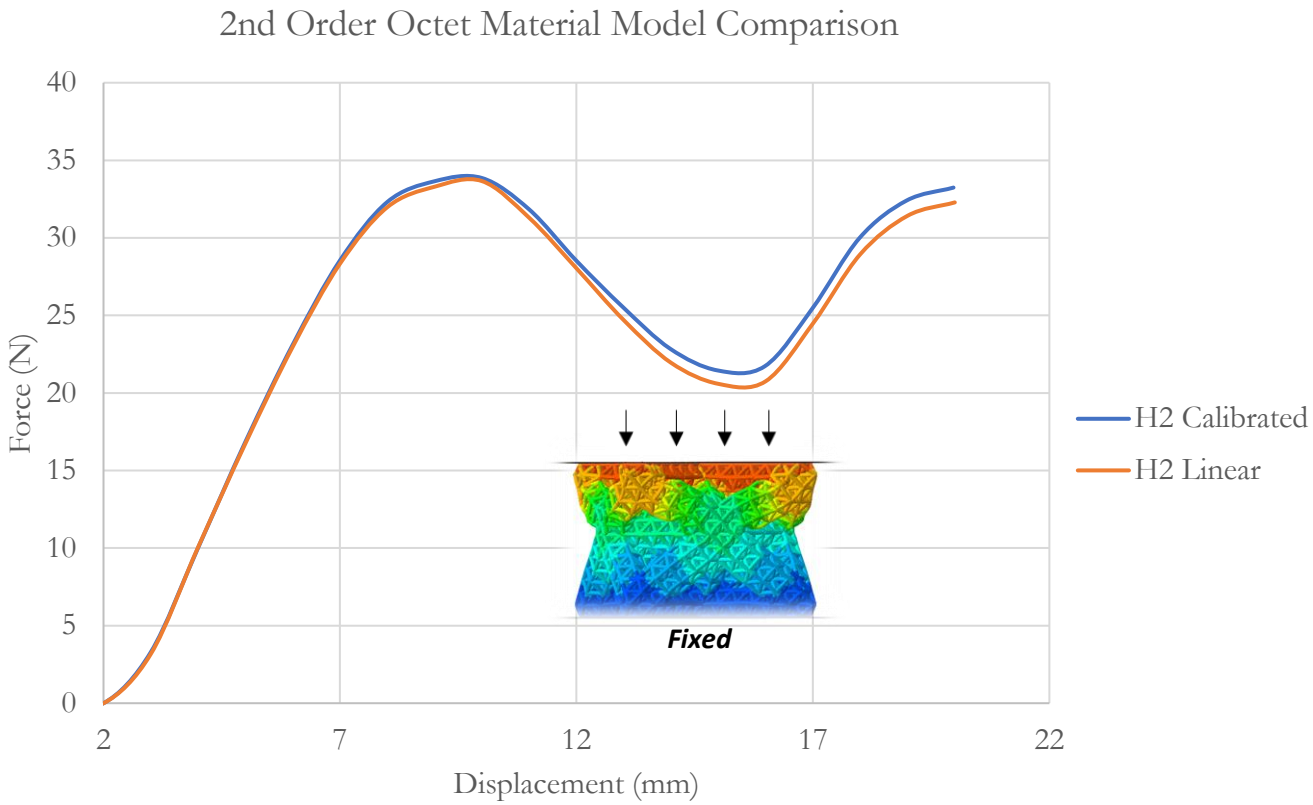

Figure 13: FEA material model comparison of linear elastic versus calibrated model using stress-strain data

2.3 Fabrication Procedure

Due to the intricate geometry of hierarchical lattices, fabrication was done with additive manufacturing using Stereolithography 3D printing technique (also known as SLA). Stereolithography is a form of 3D printing technology used for creating models, prototypes, patterns, and production parts in a layer by layer fashion using photochemical processes by which light causes chemical monomers and oligomers to cross-link together to form polymers [14].

The Form 2 printer was used in this project to fabricate the specimens (Figure 14). The flexible resin from FORMLAB is the material used with the Form 2 printer due to its high-performance dampening and cushioning effect. After the printing is done, the specimens were placed in the freezer to harden, this facilitates the removal of the support, and makes it easier compared to the rubbery state.

(a) (b) (c)

Figure 14: SLA 3D printing, (a) Form 2 3D printer, (b)(c) 3D printed specimens

2.4 Experimental Testing Setup

In order to validate FEA results, a compression testing was conducted for all fabricated specimens. The specimens were tested under a quasi-static compression at a rate of 7 mm/s (low strain rate), compressed to 50% strain (similar to FEA boundary conditions). An Instron 3343 testing machine was used in this experiment (Figure 15).

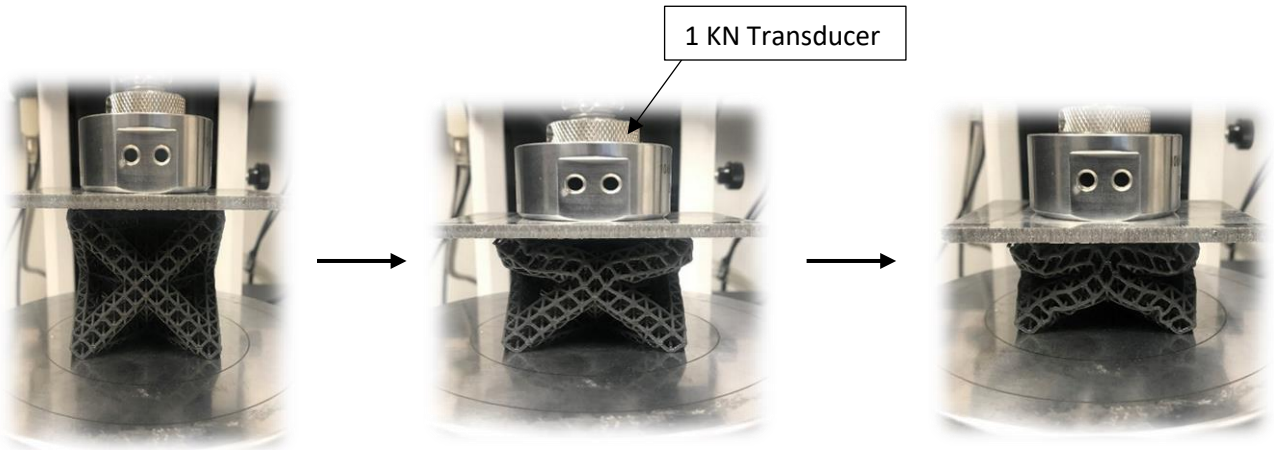

Figure 15: Compression testing using an Instron machine

CHAPTER III: FEA RESULTS AND DISCUSSION

In this chapter, the energy-absorption performance of hierarchical lattices will be investigated. In section 3.1, the significance of introducing a hierarchy on energy absorption will be demonstrated. In section 3.2, the effect of changing the 2nd order unit-cell geometry on energy absorption will be explored. Section 3.3 compares the energy absorption performance when changing the 2nd order unit cells orientation to 45-degrees. In section 3.4, the effect of manipulating the truss's cross-sectional geometry on energy absorption will be discussed.

3.1 Effect of Hierarchical Order on Energy Absorption

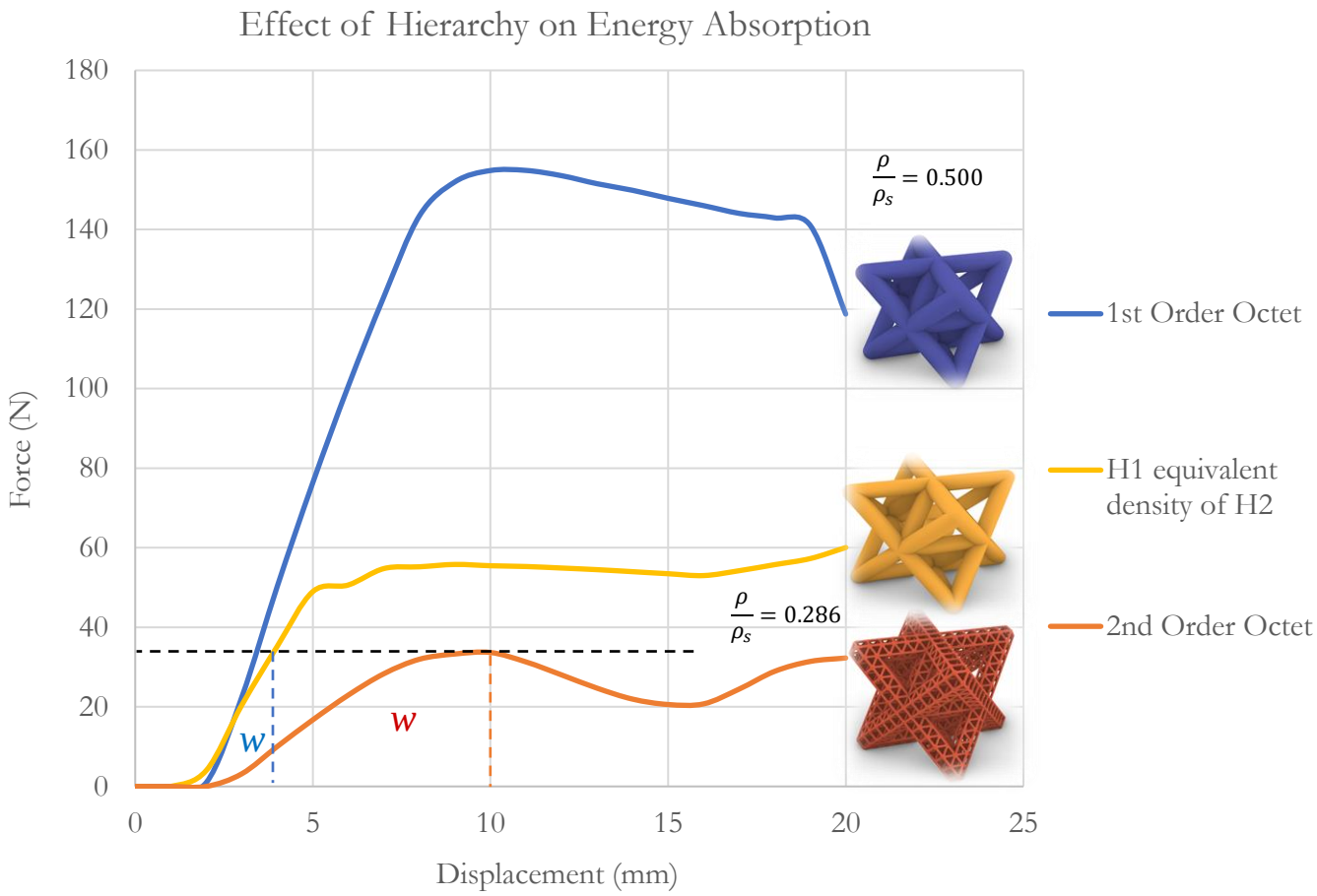

Figure 16: Effect of hierarchical order on energy absorption

Figure 16 above demonstrates the relationship between the force and the displacement for three different lattices. From each plot, one can deduce the stiffness K of each structure as $K = \frac{\Delta F}{\Delta x}$, and the energy absorbed during the low velocity (20 mm/s) compression as $W = \int F\, dx$.

From Figure 16, it can be seen that the 2nd order Octet has a larger energy absorption capacity under low loads, and up to 35 N. The 2nd order Octet experiences the plateau stress regime at an early stage compared to the 1st order Octet. This is preferable compared to the linear behavior of the 1st order Octet. This is because in the 2nd order lattice the energy is dissipated through the buckling effect of the trusses, and the friction between trusses upon interaction; and this happens within the plateau region, while the transmitted force remains constant during the impact. In the linear region of the 1st order lattice, the energy of the impact is not dissipated as much as the 2nd order, and mostly transmitted throughout the body along the linear region of the graph.

The relative density $\frac{\rho}{\rho_s}$ of the 2nd order lattice is about 0.286, ρ_s is defined as the density of the solid material, and ρ is the density of the structure of interest. One can claim that the high energy absorption performance is a result of a lower relative density, which causes the material to be softer, And thus be more effective in energy absorption applications; However, in Figure 16, the 1st order (H1) Octet with an equivalent density of a 2nd order (H2) Octet is observed to be stiffer than the 2nd order Octet , and has a lower energy absorption performance compared to the 2nd order lattice. Table 2 below summarizes the energy absorbed of each lattice at the 15 N load mark.

Lattice Design	**Energy absorbed @ 35 N**
1st order Octet (H1)	0.06 J
2nd order Octet (H2)	0.28 J
H1 same relative density as H2	0.07 J

Table 2: Effect of hierarchy on energy absorption

3.2 Effect of H2 Unit Cell Geometry on Energy Absorption

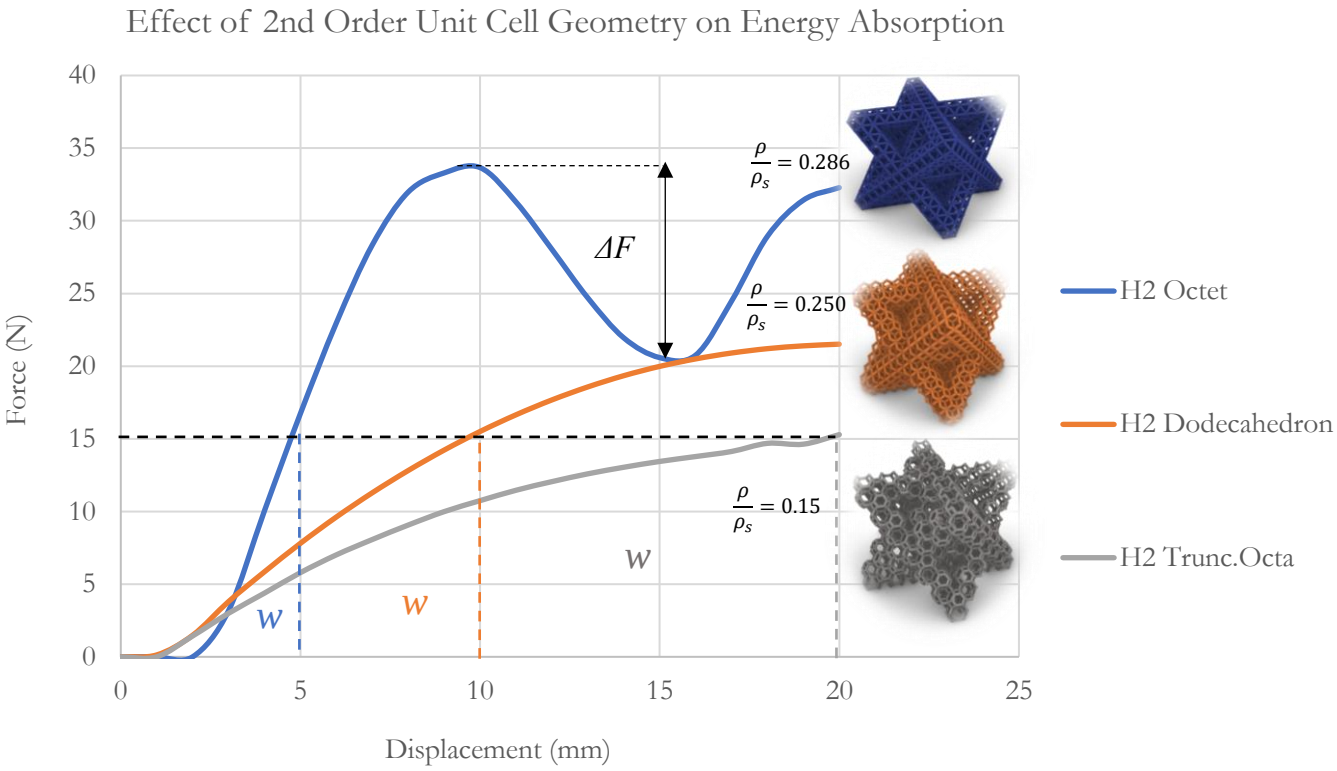

Figure 17: Effect of 2nd order unit cell geometry on Energy absorption

Figure 17 demonstrates the effect of cell geometry of the 2nd order cells on the energy absorption. It can be seen that by varying the 2nd order unit cell geometry, we can alter the stiffness and the energy absorption performance of the lattice. The 2nd order Octet demonstrated severe buckling behavior between the 10 mm and the 15 mm displacement marks, shown as ΔF in Figure 17. The 2nd order Dodecahedron and Truncated Octahedron exhibited a foam-like behavior, with a smooth continuous nonlinear deformation throughout the 50% strain-imposed boundary condition.

2nd Order Cell Geometry	Energy Absorbed @ 15 N	Volumetric Efficiency Factor η @ 15 N
Octet	0.03 J	0.03
Dodecahedron	0.08 J	0.12
Trunc.Octa	0.18 J	0.30

Table 3: Energy absorption and volumetric efficiency of hierarchical lattices

Comparing the energy absorption performance of each lattice, the H2 Truncated Octahedron curve covers a larger area than the H2 Dodecahedron lattice at the 15 N mark, and the volumetric efficiency of H2 Trunc.Octa is higher than that of H2 Dodecahedron, we conclude that the H2 Truncated Octahedron is the superior option for energy absorption applications. While the H2 Octet can serve as a viable option for higher loads scenarios due to its higher stiffness, depending on the impact force. The energy absorption efficiency is calculated using equation (1)

$$\eta = \frac{\int_0^{\varepsilon} F \, d\varepsilon}{Max(F(\varepsilon))} \qquad (1)$$

The results are demonstrated in Table 3 above, it can be inferred that efficiency decreases for those lattices with the delayed flat plateau region.

Lattice Design	Volumetric Efficiency Factor η @ 50% strain (20 mm displacement)
H2 Octet	0.35
H2 Dodecahedron	0.32
H2 Trunc.Octa	0.30

Table 4: Volumetric efficiency factors at 50% strain of hierarchical lattices

A comparison was done between the three hierarchical lattices of interest. The volumetric efficiency factor was calculated at a strain of 50%. The results are shown in Table 4 above. One can notice that the volumetric efficiency factors evaluated at 50% strain in Table 4 are different from the values in Table 3 evaluated at 15 N. This indicates that the energy absorption efficiency is not just a function of geometry, but also affected by the load or strain applied.

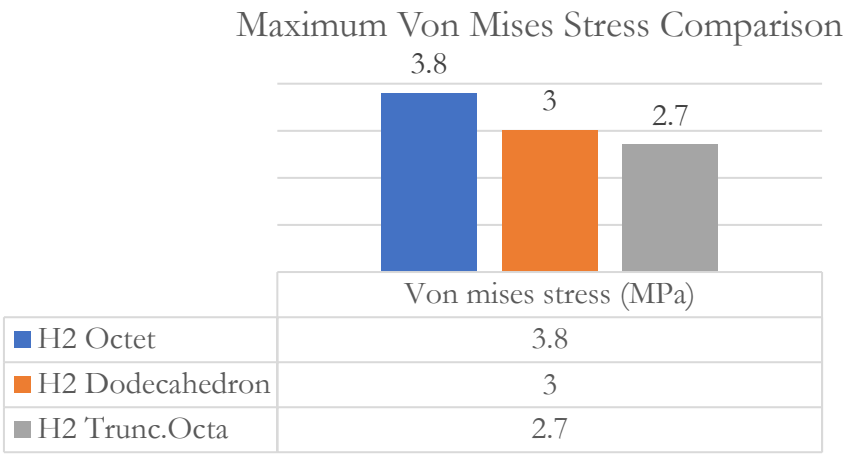

Figure 18: Maximum von mises stress in three H2 lattices

In Figure 18 above, a comparison of the maximum von misses stress in each lattice is demonstrated to aid the argument of Figure 17 above. The trend that can be noted here is that the lattice with the highest von mises stress (H2 Octet) corresponds to the lattice with the lowest energy absorption performance in Figure 17. Similarly, the lattice with the lowest von mises stress (H2 Trunc.Octa) corresponds to the lattice with highest energy absorption performance.

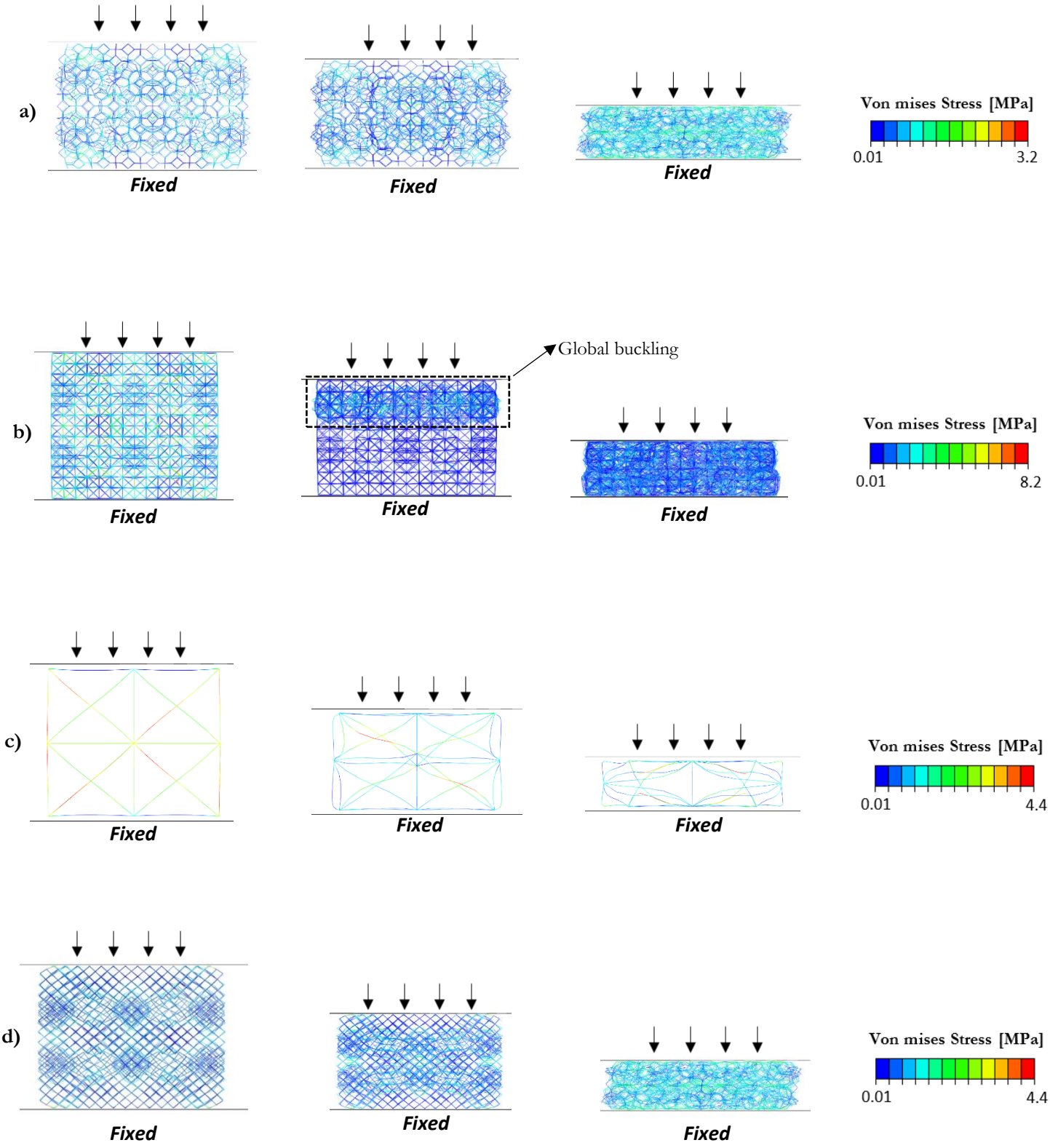

Figure 19: FEA Von mises stress contours, (a) H2 Trunc.Octa, (b) H2 Octet, (c) H1 Octet, (d) H2 Dodecahedron

It's important to note that the highest stress occurs at a very minimal local points, and the von mises stresses at other regions of the lattice is much smaller than the highest local von mises stress. This can be seen from the color distribution of the stress contours in Figure 19; and hence the linear elastic model was used in this study. In section 2.2 Figure 12, it was established that the plastic deformation region starts at about 4 MPa, the results from Figure 19 above indicates that the lattices under investigation are operating under the linear elastic model, and experiencing a very negligible plastic deformation, allowing the lattices to be used again. Detailed von mises stress contours of all lattices in this analysis can be seen in Appendix A. Moreover, Figure 19 (b) above demonstrates a global buckling in the lattice, this explains the ΔF observed of the H2 Octet in Figure 17 between the 10 mm and the 15 mm marks.

3.3 Effect of H2 Unit Cell Orientation on Energy Absorption

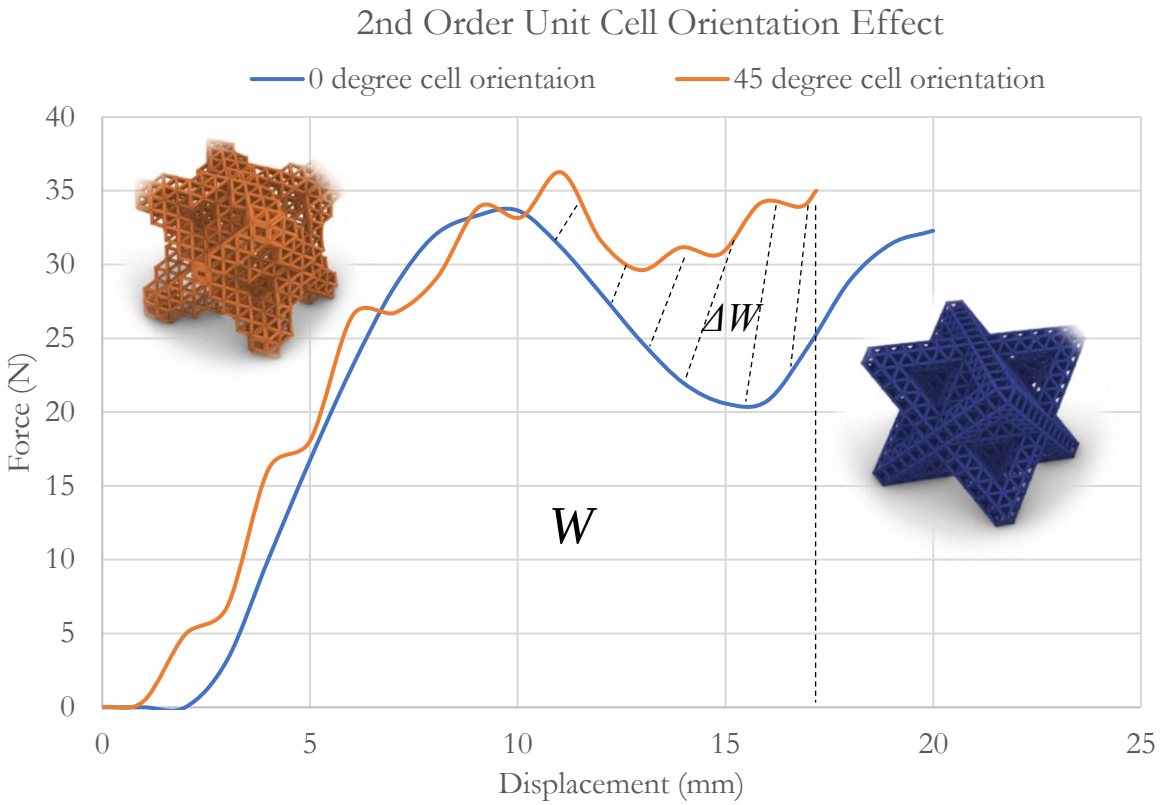

Figure 20: Effect of 2nd order cell orientation on energy absorption

In Figure 20 above, a comparison between two H2 Octet lattices is shown. One with the H2 cells making a 0-degree angle with the XY plane, the second one with the H2 cells making a 45-degree angle with XY plane. The XY plane is defined as a horizontal flat plane. The behavior of the second order unit cell orientation was investigated under compression. The 45-degree oriented H2 cells showed a less severe global buckling behavior between the 10 mm and 15 mm displacement marks, but a higher local truss-buckling effect demonstrated as ripples along the curve. The overall energy absorption capacity of the H2 45d Octet is larger than its H2 Octet counterpart, about 20% improvement. This can be seen in the hatched area in Figure 20.

3.4 Effect of H2 Cross-Sectional Geometry of Trusses

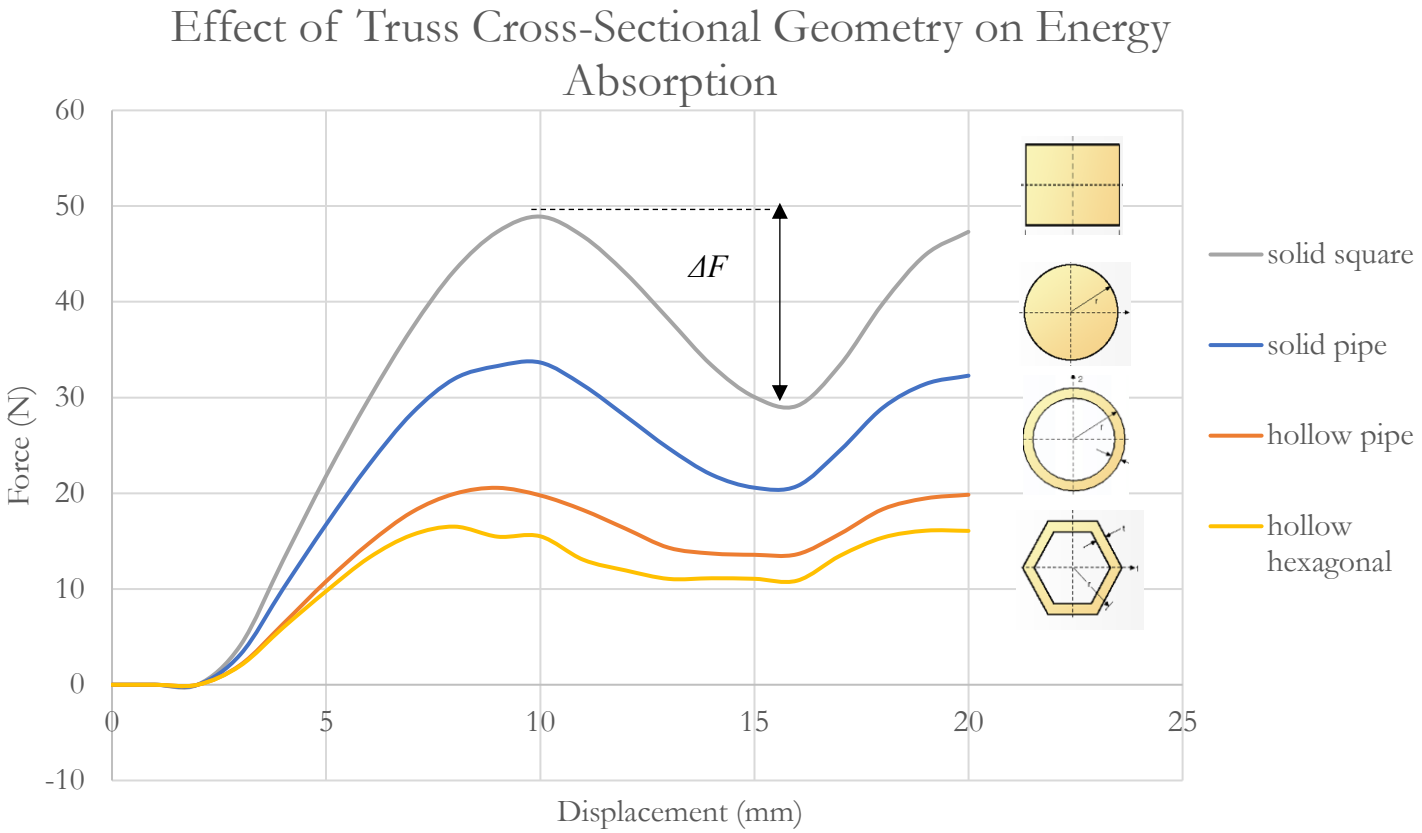

Figure 21: Effect of truss cross-sectional geometry on energy absorption

In Figure 21, the effect of changing the truss cross-sectional geometry is studied. The geometric description of each cross section can be found in Appendix B. The results showed that for the hollow cross sections, such as the hollow pipe and the hollow hexagonal shape, the buckling occurs in a consistent manner, with no abrupt changes in force, this can be seen in the region between the 10 mm to the 18 mm displacement marks. In comparison, the solid counterparts such as the solid circular pipe, and the solid square, exhibited an abrupt change in the force demonstrated by ΔF in the plot. The largest abrupt change in the force (ΔF) corresponds to the stiffest lattice with trusses that have solid circular, and solid square cross-sectional geometry, Table 5 below summarizes the findings.

According to Newton's second law of motion, the change in force is interpreted as a change in the acceleration rate, which is not something preferable when designing energy-absorption structures.

The lattices with the trusses of hollow cross-sectional geometry recorded the highest energy absorption efficiency, this is because the weaker hollow trusses are more prone to bucking, and thus the lattice will absorb more energy upon collapsing.

Cross section Geometry	**Stiffness K**	**Max Magnitude of the ΔF**	**Volumetric energy absorption efficiency η @ 50% strain (20 mm displacement)**
Solid square	8.8 N/mm	20 N	0.33
Solid circular	6.6 N/mm	12 N	0.35
Hollow circular	4 N/mm	5 N	0.40
Hollow hexagonal	4 N/mm	5 N	0.40

Table 5: Summary of stiffness, magnitude of ΔF, and Volumetric energy absorption efficiency η for various truss cross sectional geometries on a H2 Octet lattice

3.5 Analytical Solution

The analytical solution for the 1st order and the 2nd order Octet lattices were investigated. To obtain the effective relative density of a 2nd order Octet lattice we use equation (2) [18].

$$\bar{\rho}^{(Octet)}{}_2 = \frac{36Q-92}{Q^3}\left[\frac{25\sqrt{2}\pi}{16}\left(\frac{d_1}{l_1}\right)^2 - (5.922\left(\frac{d_1}{l_1}\right)^3\right] \quad (2)$$

The relative density of the 1st order is obtained the conventional way:

$$\rho_1 = \frac{m}{V} \quad (3)$$

Using the results of equation (2) and (3), we obtain the stiffness for both the 1st and 2nd order Octet lattices by evaluating equation (4) and (5) [6]. Where C in equation (4) is a proportionality constant close to unity for $\frac{\rho}{\rho_s} < 0.3$, E_s is the stiffness of the solid constituent material, and ρ_s is the density of the solid constituent material. Table 6 summarizes all the parameters used in the analytical solution

$$E_{2nd\ order} = E_s * C * \left(\frac{\rho_{2nd\ order}}{\rho_s}\right)^2 \quad (4)$$

$$E_{1st\ order} = E_s * C * \left(\frac{\rho_1}{5}\right) \quad (5)$$

Table 6: Parameters of Analytical Solution

Symbol	Description	Value
d_1	Diameter of second order truss	1 mm
l_1	Length of second order truss	4.5 mm
Q	Number of unit cells across L/2	7
ρ_s	Density of solid material	1.2 g/cc
ρ_1	Density of 1st order lattice	0.5 g/cc
$\bar{\rho}^{(Octet)}{}_2$	Density of 2nd order lattice	0.13 g/cc
E_s	Stiffness of solid material	12 MPa
$E_{1st\ order}$	Stiffness of 1st order lattice	1.2 MPa
$E_{2nd\ order}$	Stiffness of 2nd order lattice	0.14 MPa

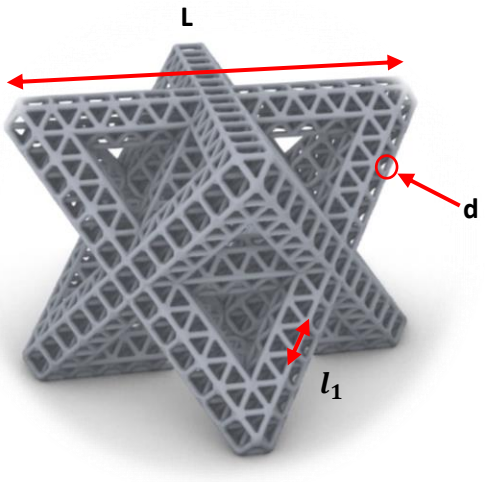

As a method of validation, we compare the ratio of stiffness $\frac{E_1}{E_2} = \frac{E_{1st\ order}}{E_{2nd\ order}}$ for the analytical solution and the FEA solution as discussed in section 3.1. (E_1, E_2) values for the analytical solution are obtained from equation (3) and (4). While (E_1, E_2) values for the FEA solution were obtained from the linear slope of the graph using $E = K = \frac{\Delta F}{\Delta x}$ for macro scale structures. Figure 22 depicts the stiffness ratio of H1 and H2 lattices obtained using the FEA and the analytical solution. The difference is within 7.45% which can be attributed to contact and material model approximation.

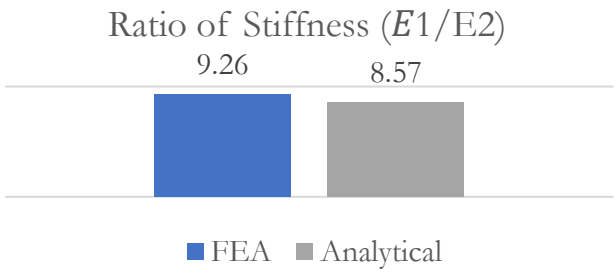

Figure 22: Ratio of stiffness between H1 and H2 Octet (Analytical and FEA)

3.6 Experimental Testing

In Figure 23 and 24 below, a force-displacement plot demonstrates the difference in stiffness and energy absorption performance between a 1st order (Figure 23) and a 2nd order Octet lattice (Figure 24). Quantitively, the stiffnesses observed from the experimental plots are different than the ones observed from the FEA results; that's because the material used in the experimental testing is "flexible resin", and has different mechanical properties compared to the TPU model used in FEA. The ratio of the stiffness ended up being $\frac{E_1}{E_2} = \frac{E_{1st\ order}}{E_{2nd\ order}} = 17$. A source of error that was noticed and could elevate the ratio $\frac{E_{1st\ order}}{E_{2nd\ order}}$ are fabrication defects in the 2nd order lattice, like broken trusses, which

causes the structure to be softer than what it is supposed to be. Another possible source of error is the assumption that flexible resin behaves in a linear elastic manner. In figure 24, experimental data is compared against simulation data implementing various approximated stiffness values for flexible resin. Qualitatively, the buckling behavior shown in Figure 24 is similar to the FEA result discussed in section 3.2.

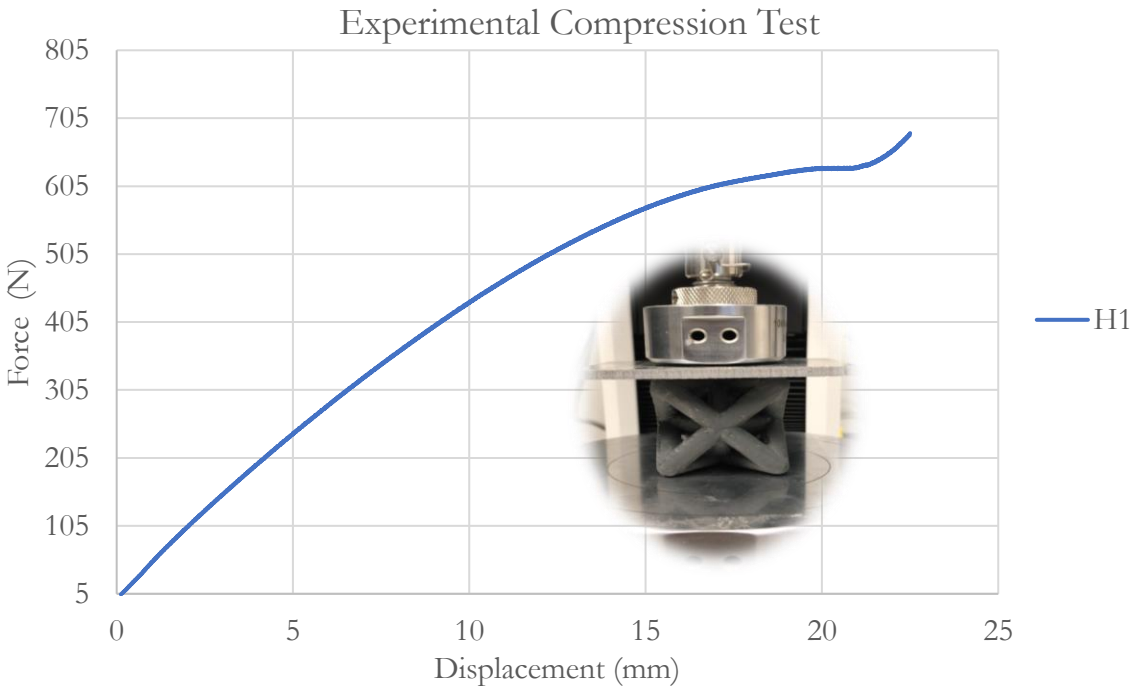

Figure 23: Experimental force-displacement curve of H1 Octet

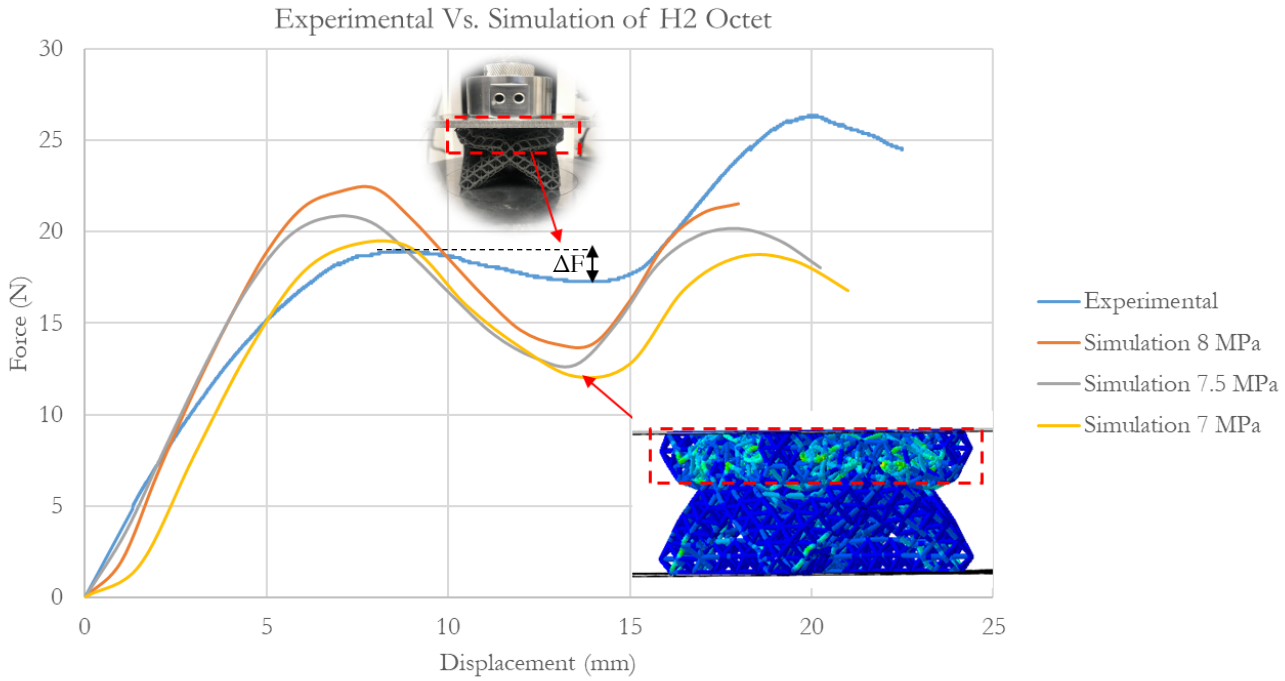

Figure 24: Experimental and simulation (linear) plots of H2 Octet

CHAPTER IV: CONCLUSION AND FUTURE WORK

This study presented hierarchical lattices as one way to create high-efficiency energy absorption structures inspired from biological structures. With the continuous advancements in computer-aided design and additive manufacturing, such complicated designs are now easily attainable. This study investigated the following effects on the energy-absorption performance of hierarchical lattices:

1. The effect of introducing a hierarchy to an Octet lattice
2. The effect of altering the 2nd order unit cell geometry
3. The effect of 2nd order unit cells orientation with respect to the base XY plane
4. The effect of changing the lattice trusses cross-sectional geometry

It was concluded that by introducing a hierarchy:

- The energy absorption performance of the lattice increases four to five times.
- Introducing a hierarchy increases the number of trusses in the lattice that are prone to buckling, which is one of the main mechanisms for energy absorption.
- Lowering the relative density by itself did not provide the best energy absorption performance, it was deduced that the energy absorption is not just a function of relative density, but also of geometry.
- Stiffness by itself doesn't help in predicting whether a lattice will be a good candidate in an energy-absorption application, one has to study other factors such as the force-displacement, and the volumetric energy absorption efficiency at the load or strain of interest.
- Changing the 2nd order unit cell geometry affected the stiffness and the energy absorption performance of the lattices, with the H2 Trunc.Octa lattice demonstrating the best energy absorption performance under low loads when compared to the H2 Octet and the H2

Dodecahedron lattices. However, over the full range of 50% strain, all hierarchical lattices demonstrated similar efficiency, with the H2 Octet showing the highest volumetric energy absorption.

- Changing the 2nd order unit cells orientation by tilting the cells 45 degrees with respect to the base XY plane caused a minor increase in the stiffness, and 20% increase in energy absorption capacity. It was also noted that the hollow trusses performed better than the solid trusses in terms of energy absorption; reducing the material in the trusses reduces the stiffness of the trusses, and therefore facilitates the buckling behavior.

The future work of this study aims at implementing topology optimization algorithms on hierarchical lattices in order to obtain an optimized energy absorption lattice for a specific load scenario. In addition, since most energy absorption applications are associated with high velocity impacts, such as protection equipment in sports and crashworthiness applications, the dynamic behavior of the hierarchical structures should be explored further with high strain-rates.

BIBLIOGRAPHY

[1] Lim, Jongsoo, et al. "A Study on Energy Absorption Characteristic and Head Injury Performance According to The Characteristic of Countermeasures and Space Between Interior and Body Structures." 2013, https://trid.trb.org/view/1361107.

[2] Chiu, Hung-Ta, and Tzyy-Yuang Shiang. "Effects of Insoles and Additional Shock Absorption Foam on the Cushioning Properties of Sport Shoes." Journal of Applied Biomechanics, vol. 23, no. 2, 2007, pp. 119–127., doi:10.1123/jab.23.2.119.

[3] Clough, Eric C., et al. "Elastomeric Microlattice Impact Attenuators." SSRN Electronic Journal, 2019, doi:10.2139/ssrn.3427465.

[4] Alkhatib, Sami E., et al. "Deformation Modes and Crashworthiness Energy Absorption of Sinusoidally Corrugated Tubes Manufactured by Direct Metal Laser Sintering." Engineering Structures, vol. 201, 2019, p. 109838., doi:10.1016/j.engstruct.2019.109838.

[5] Chen, Pu-Woei, and Ya-Yun Lin. "Evaluation on Crashworthiness and Energy Absorption of Composite Light Airplane." Advances in Mechanical Engineering, vol. 10, no. 8, 2018, p. 168781401879408., doi:10.1177/1687814018794080.

[6] Gibson, Lorna J., and Michael F. Ashby. Cellular Solids: Structure and Properties. Cambridge Univ. Press, 2010.

[7] Cui, Liang, et al. "Designing the Energy Absorption Capacity of Functionally Graded Foam Materials." Materials Science and Engineering: A, vol. 507, no. 1-2, 2009, pp. 215–225., doi:10.1016/j.msea.2008.12.011.

[8] Linul, Emanoil, et al. "Energy - Absorption and Efficiency Diagrams of Rigid PUR Foams." Key Engineering Materials, vol. 601, 2014, pp. 246–249., doi:10.4028/www.scientific.net/kem.601.246.

[9] Bertoldi, Katia. "Harnessing Instabilities to Design Tunable Architected Cellular Materials." Annual Review of Materials Research, vol. 47, no. 1, Mar. 2017, pp. 51–61., doi:10.1146/annurev-matsci-070616-123908

[10] Jin, Nan, et al. "Failure and Energy Absorption Characteristics of Four Lattice Structures under Dynamic Loading." Materials & Design, vol. 169, 2019, p. 107655., doi:10.1016/j.matdes.2019.107655.

[11] Tsang, H.h., and S. Raza. "Impact Energy Absorption of Bio-Inspired Tubular Sections with Structural Hierarchy." Composite Structures, vol. 195, 2018, pp. 199–210., doi:10.1016/j.compstruct.2018.04.057.

[12] Fischer, S.F., et al. Pummelos as concept generators for biomimetically inspired low weight structures with excellent damping properties. 2010. P.O. Box 101161, Weinheim, D-69451, Germany: Wiley-VCH Verlag.

[13] Meza, Lucas R., et al. "Resilient 3D Hierarchical Architected Metamaterials." Proceedings of the National Academy of Sciences, vol. 112, no. 37, Jan. 2015, pp. 11502–11507., doi:10.1073/pnas.1509120112.

[14] "US4575330A - Apparatus for Production of Three-Dimensional Objects by Stereolithography." Google Patents, Google, patents.google.com/patent/US4575330A/en

[15] Ismail, Muhammad F., et al. "Low Velocity Impact Behaviour and Post-Impact Characteristics of Kenaf/Glass Hybrid Composites with Various Weight Ratios." Journal of Materials Research and Technology, vol. 8, no. 3, 2019, pp. 2662–2673., doi:10.1016/j.jmrt.2019.04.005.

[16] Harne, Ryan L., and K. W. Wang. Harnessing Bistable Structural Dynamics: for Vibration Control, Energy Harvesting and Sensing. Wiley, 2017.

[17] Mehta, P., Solis Ocampo, J., Tovar, A., and Chaudhari, P., "Bio-Inspired Design of Lightweight and Protective Structures," SAE Technical Paper 2016-01-0396, 2016, doi:10.4271/2016-01-0396.

[18] Yin, Sha, et al. "Effects of Architecture Level on Mechanical Properties of Hierarchical Lattice Materials." International Journal of Mechanical Sciences, vol. 157-158, 2019, pp. 282–292., doi:10.1016/j.ijmecsci.2019.04.051.

[19] Yuan, Shangqin, et al. "3D-Printed Mechanical Metamaterials with High Energy Absorption." Advanced Materials Technologies, vol. 4, no. 3, Apr. 2018, p. 1800419., doi:10.1002/admt.201800419.

[20] Cetin, Erhan, and Cengiz Baykasoğlu. "Energy Absorption of Thin-Walled Tubes Enhanced by Lattice Structures." International Journal of Mechanical Sciences, vol. 157-158, 2019, pp. 471–484., doi:10.1016/j.ijmecsci.2019.04.049.

[21] Al-Saedi, Dheyaa S.j., et al. "Mechanical Properties and Energy Absorption Capability of Functionally Graded F2BCC Lattice Fabricated by SLM." Materials & Design, vol. 144, 2018, pp. 32–44., doi:10.1016/j.matdes.2018.01.059.

[22] Tancogne-Dejean, Thomas, et al. "Additively-Manufactured Metallic Micro-Lattice Materials for High Specific Energy Absorption under Static and Dynamic Loading." Acta Materialia, vol. 116, 2016, pp. 14–28., doi:10.1016/j.actamat.2016.05.054.

[23] J.A. Newman, International Conference on the Biomechanics of Impact (IRCOBI), 1986.

[24] BSI, EN 14572:2005: High performance helmets for equestrian activities, British Standards Institution, London, 2005.

APPENDIX

A. FEA Stress Contour Plots

(A1) 1st order Octet von mises plot

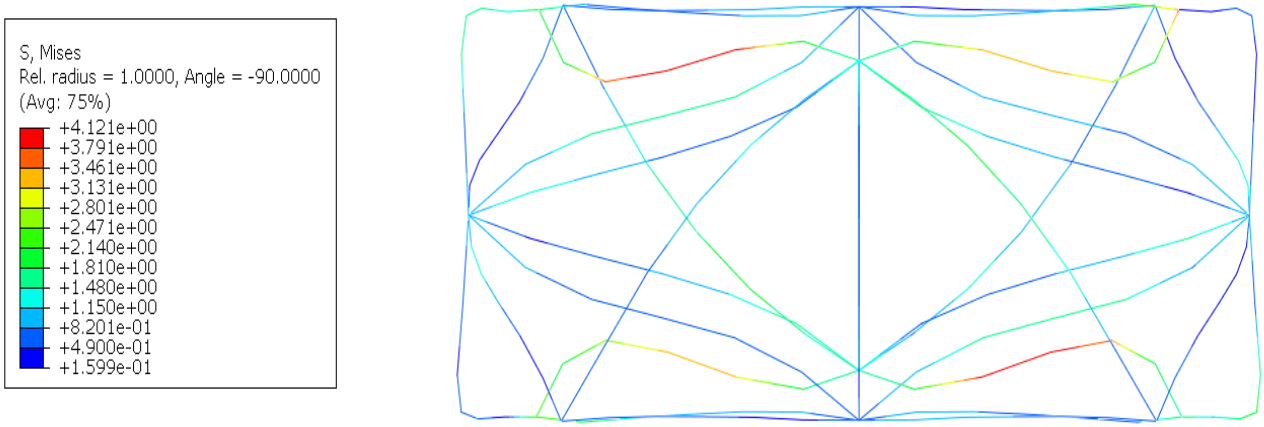

(A2) 2nd order Octet von mises plot

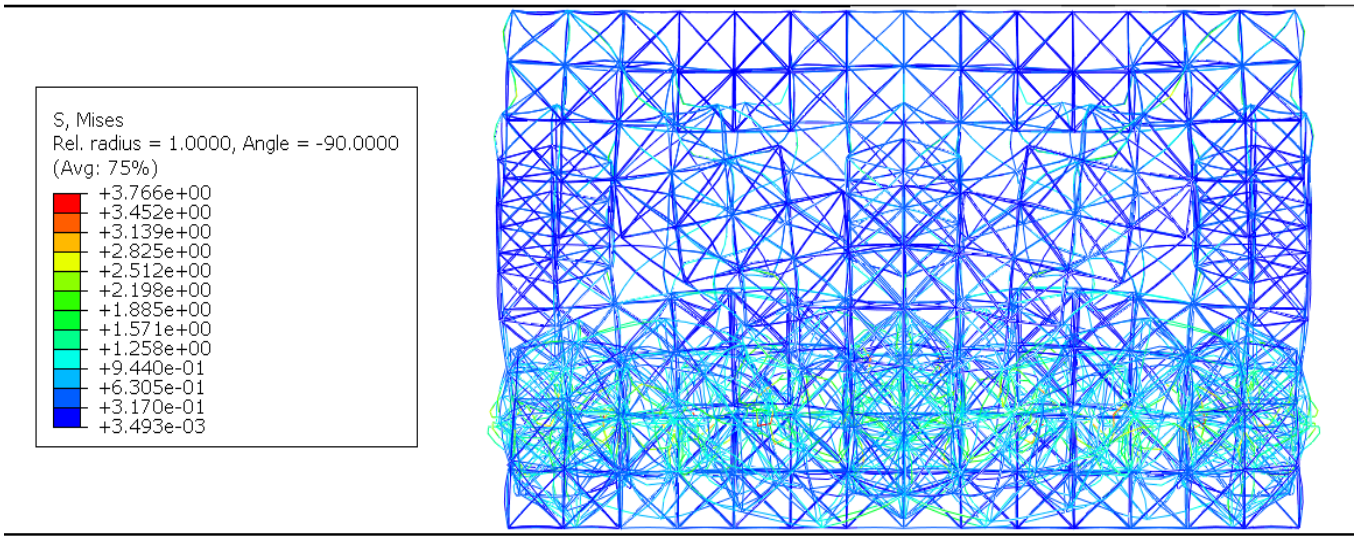

(A3) 2nd order Octet 45 degrees orientation von mises plot

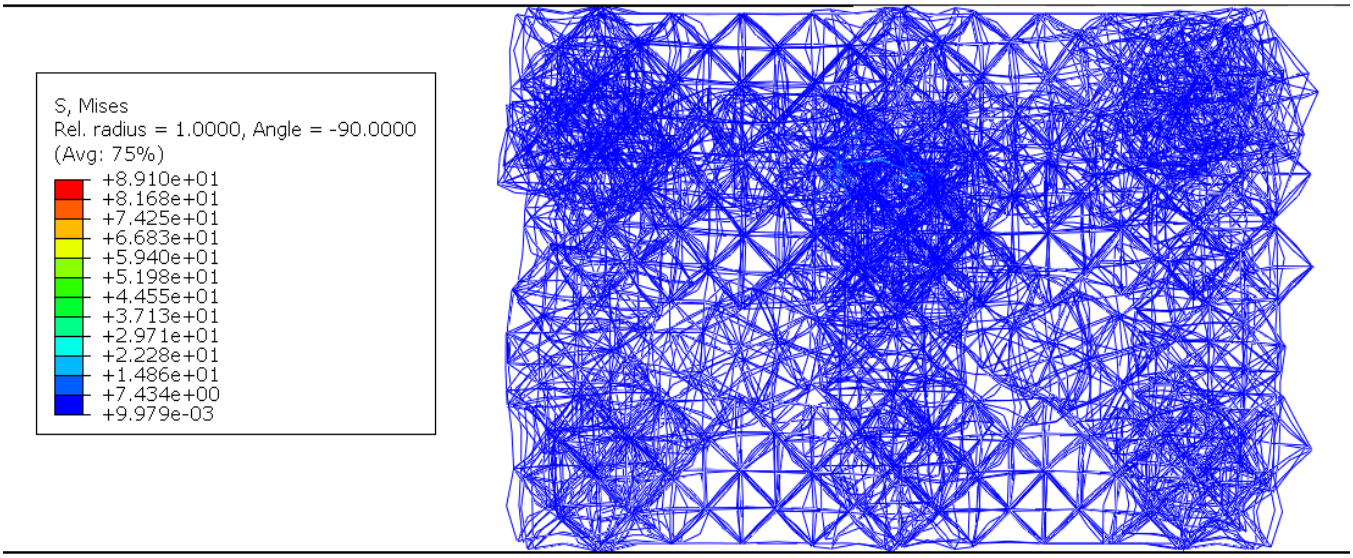

(A4) 2nd order truncated octahedron von mises plot

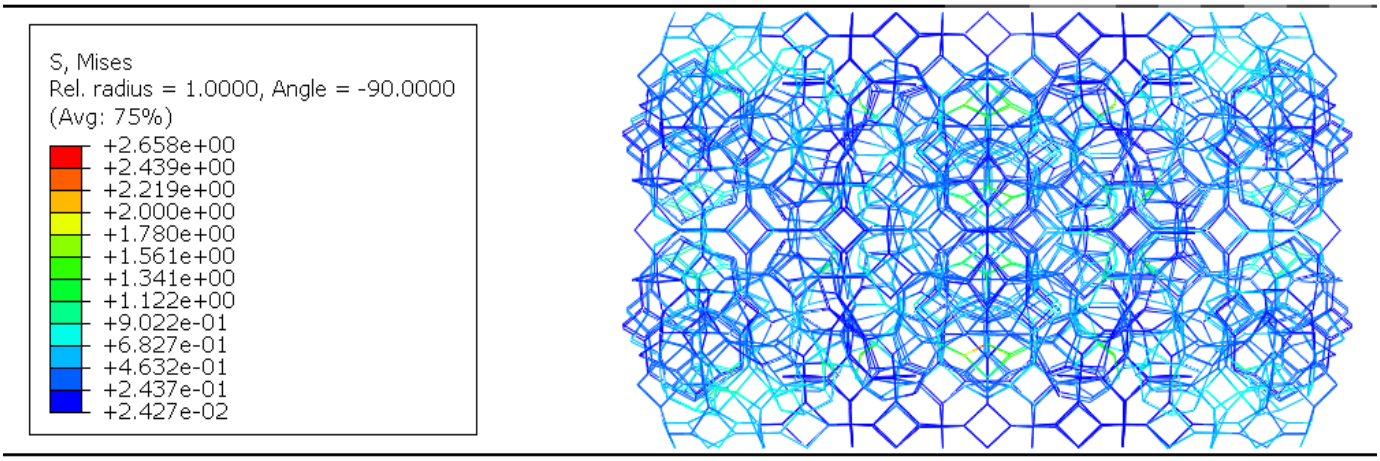

(A5) 2nd order dodecahedron von mises plot

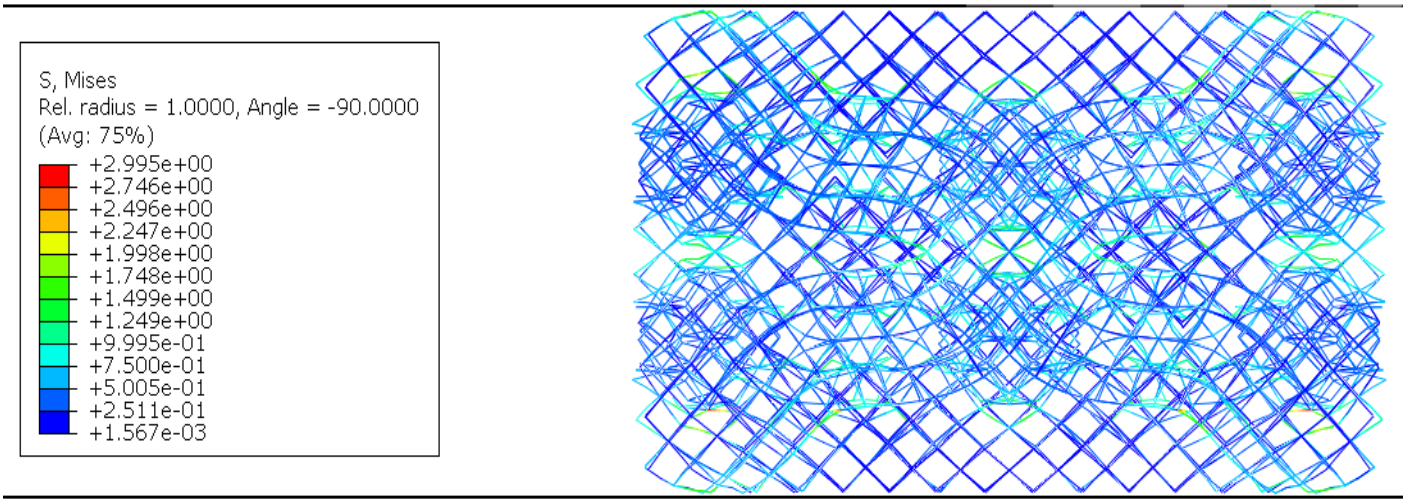

B. Geometric Parameters of Truss Cross-Sections

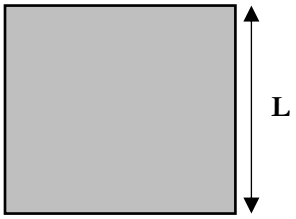

Solid square

L=1 mm

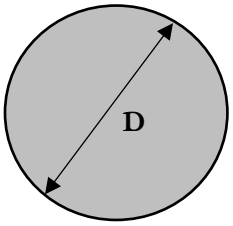

Solid circular

D=1 mm

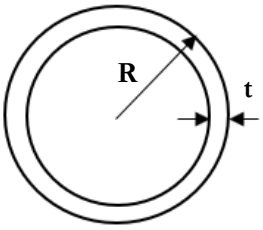

Hollow circular

R=0.5 mm

t=0.125 mm

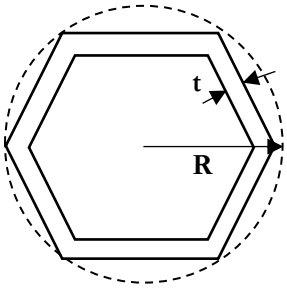

Hollow circular

R=0.5 mm

t=0.125 mm